Isolation of the Yeast Nuclear Pore Complex

Michael P. Rout and Günter Blobel

Laboratory of Cell Biology, Howard Hughes Medical Institute, The Rockefeller University, New York, New York 10021

Abstract. Nuclear pore complexes (NPCs) have been isolated from the yeast Saccharomyces. Negative stain electron microscopy of the isolated NPCs and subsequent image reconstruction revealed the octagonal symmetry and many of the ultrastructural features characteristic of vertebrate NPCs. The overall dimensions of the yeast NPC, both in its isolated form as well as in situ, are smaller than its vertebrate counterpart. However, the diameter of the central structures are similar. The isolated yeast NPC has a sedimentation coefficient of ~310 S and an M_r of ~66 MD. It retains all but one of the eight known NPC proteins. In addition it contains as many as 80 uncharacterized proteins that are candidate NPC proteins.

NUCLEAR pore complexes (NPCs)[1] occur at circular apertures in the nuclear envelope where the inner and outer nuclear membranes are joined, and mediate nucleocytoplasmic exchanges. Their ultrastructure has been well studied, and mapped to a resolution of better than 10 nm in Xenopus. They are cylindrical supramolecular assemblies displaying octagonal symmetry, with their eightfold axes perpendicular to the plane of the nuclear envelope (for review see Akey, 1992). NPCs are found in all eukaryotic cells and their general morphology appears to be highly conserved between evolutionary divergent phyla. The role of NPCs in nucleocytoplasmic transport has been studied intensively in recent years. The presence of the NPC limits the functional size of passive diffusion across the nuclear envelope to ~9–10 nm. However, proteins and RNAs larger than this can be rapidly transported through the center of each NPC by an active, vectorial, signal-dependent process (for reviews see Franke, 1974; Maul, 1977; Gerace and Burke, 1988; Miller et al., 1991; Forbes, 1992).

The detailed ultrastructure of vertebrate NPCs has been well documented, particularly in isolated nuclear envelope and NPC–lamina fractions, which are free of material that normally obscures the NPC. Ultrastructural analysis of nuclear envelopes from Xenopus oocytes has shown that the NPC is composed of several distinct structural regions. The core of the NPC is built from three coaxial rings, each around 120 nm in diameter; the outer and inner rings are coplanar with the outer and inner nuclear membranes, respectively, and have an eightfold symmetry similar to that of the central ring, which is made of eight radial spokes. Each spoke is divided perpendicular to its axis into three domains. Residing centrally within and supported by this spoke-ring complex is the plug, believed to be a coaxial tube (termed the "transporter") through which macromolecules are actively translocated. Pairs of radial arms interconnect adjacent spokes within the lumen of the nuclear envelope, to form a continuous ring coplanar with and surrounding the central spoke ring (Unwin and Milligan, 1982; Akey, 1989, 1990; Hinshaw et al., 1992; Akey and Radermacher, 1993). Eight perpendicular filaments extend from both the nuclear and cytoplasmic surfaces. The nuclear filaments are linked by a distal ring to form the so-called "baskets" (Ris, 1990, 1991; Jarnik and Aebi, 1991; Goldberg and Allen, 1992).

Little is known about the composition of the NPC. The biochemical characterization of NPC proteins has used material derived primarily from rat liver nuclei. Procedures producing partially enriched fractions of NPCs from these nuclei have been described (Dwyer and Blobel, 1976), though intact NPCs have not been separated from the attached lamina. Generally, proteins associated with the NPC have been identified in vertebrates either immunochemically or by subfractionation of nuclear envelopes (Gerace et al., 1982; Davis and Blobel, 1986, 1987; Snow et al., 1987; Park et al., 1987; Dabauvalle et al., 1988; Wozniak et al., 1989; Radu et al., 1993). Only four such mammalian proteins have been molecularly cloned and sequenced to date (Wozniak et al., 1989; Starr et al., 1990; Cordes et al., 1991; Carmo-Fonesca et al., 1991; Sukegawa and Blobel, 1993; Radu et al., 1993). A number of monoclonal antibodies that identify members of a family of NPC proteins in mammals also cross-react with homologous proteins in Xenopus and the yeast Saccharomyces (Davis and Blobel, 1986, 1987; Snow et al., 1987; Park et al., 1987; Dabauvalle et al., 1988; Featherstone et al., 1988; Aris and Blobel, 1989; Davis and Fink, 1990; Wente et al., 1992; Loeb et al., 1993). This cross-reactivity has been used to molecularly clone and sequence five yeast NPC proteins (Davis and Fink, 1990; Wente et al., 1992; Loeb et al., 1993), with a sixth having

Please address all correspondence to Dr. G. Blobel, Laboratory of Cell Biology, Howard Hughes Medical Institute, The Rockefeller University, New York, NY 10021.

1. *Abbreviations used in this paper:* NPCs, nuclear pore complexes; SPBs, spindle pole bodies.

been identified independently (Nehrbass et al., 1990). Two of these proteins were subsequently identified using genetic screens (Wimmer et al., 1992).

Though little is known about the detailed structure of yeast NPCs, they have similar functions to those of higher eukaryotes (Forbes, 1992). Biochemical approaches of the type successfully used in the isolation of vertebrate NPC proteins have proven more difficult in yeast. However, the production of large quantities of yeast nuclei is relatively straightforward and some progress in their subfractionation has been reported (Rozijn and Tonino, 1964; Kilmartin and Fogg, 1982; Hurt et al., 1988; Aris and Blobel, 1988, 1989; Allen and Douglas, 1989; Cardenas et al., 1990; Rout and Kilmartin, 1990). Here we describe a large scale, high yield biochemical procedure producing a highly enriched NPC fraction, that has revealed over 80 distinct candidate NPC proteins.

Materials and Methods

Buffers and Solutions

NPC buffer: 10 mM bisTris-Cl, pH 6.50, 0.1 mM $MgCl_2$, 1.0% sodium taurodeoxycholate (Sigma Chem. Co., St. Louis, MO), 10 μg/ml RNase A (Sigma Chem. Co.), 0.5 mM DTT.

bt buffer: 10 mM bisTris-Cl, pH 6.50, 0.1 mM $MgCl_2$.

bt-DMSO buffer: 10 mM bisTris-Cl, pH 6.50, 0.1 mM $MgCl_2$, 20% DMSO.

Solution P: 87.0 mg PMSF plus 1.5 mg pepstatin A, dissolved in 5 ml dry absolute ethanol.

Preparation of a Highly Enriched Nuclear Pore Complex Fraction

All solutions contained a 1:1,000 dilution of solution P unless otherwise stated. The yeast strain Saccharomyces uvarum (NCYC 74, ATCC 9080), considered a strain of *S. cerevisiae* (Mortimer and Johnston, 1986), was used due to the ease with which it can be spheroplasted (Eddy and Williamson, 1957). Crude and enriched nuclear fractions were prepared by using the method described in Rout and Kilmartin (1990, 1993) (modified from Rozijn and Tonino, 1964), except that Triton X-100 was omitted from the spheroplast lysis solution. Nuclear lysis and the separation of the lysate over a stepped sucrose gradient were exactly as described, with the crude NPC fraction being recovered from the S/1.75 M interface (Rout and Kilmartin, 1990, 1993).

The enriched NPC fraction was produced as follows. The protein concentration of the S/1.75 crude NPC fraction (above) was determined by using the Bradford protein assay (see below). Five volumes of this fraction were then diluted by the addition of one volume of ice cold NPC buffer, a 1:200 dilution of solution P, and a final concentration of 0.045 mg of heparin (sodium salt; Sigma Chem. Co.) per 1.0 mg of S/1.75 M fraction protein. The mixture was vortexed thoroughly, incubated for 15 min at 10°C, and centrifuged to remove the froth (700 *g*, 4 min, 4°C) before being loaded onto precooled SW55 tubes (Beckman Instrs., Fullerton, CA) (1.2 ml per tube), each containing 0.5 ml of 2.50 M sucrose-bt (refractive index 1.4533), 1.5 ml of 1.85 M sucrose-bt + 0.2% Triton X-100 (refractive index 1.4225), and 1.5 ml of 1.45 M sucrose-bt + 0.2% Triton X-100 (refractive index 1.4032). It should be noted that making all the sucrose solutions discussed in this method by their refractive index (measured at room temperature) was important for the success of the procedure. The sample layer was then overlayered with 0.7 ml of bt-DMSO and the tubes were centrifuged at 237,000 g_{av} for 5 h at 4°C. The tubes were unloaded from the top. The first 1.5 ml was termed the S fraction and the second 1.5 ml the S/1.45 fraction, as they contained the supernatant and the supernatant/1.45 M interface, respectively. The enriched NPC fraction was recovered in 1.5 ml from the 1.45 M/1.85 M interface, called the 1.45/1.85 fraction. The final 0.8 ml contained the 1.85 M/2.50 M interface (installed for diagnostic purposes) and was termed the 1.85/2.5 fraction.

To produce the highly enriched NPC fraction, the pooled 1.45/1.85 enriched NPC fraction was diluted with an equal volume of bt-DMSO buffer and a 1:500 dilution of solution P. 4-ml aliquots of this were each overlayered onto a Beckman SW28 centrifuge tube containing a 5-ml cushion of "1.75 M" sucrose bt-DMSO + 0.01% Tween-20 (refractive index 1.4495) and 29 ml of a continuous linear gradient of "1.20 M" sucrose (refractive index 1.4220) to "1.00 M" sucrose (refractive index 1.4120) in bt-DMSO + 0.01% Tween-20. All the tubes were then centrifuged in a Beckman SW28 rotor at 104,000 g_{av} for 24 h at 4°C. After centrifugation a faint white band was visible around the "1.20 M"/"1.75 M" interface in each tube; its position was marked. Each gradient was unloaded from the top; the first 9 ml was termed fraction #1 and the second 9 ml, fraction #2. The third 9 ml, fraction #3, was collected to within ~5 mm above the marked band. The fourth fraction was the 10 ml containing the marked band and the "1.20 M"/"1.75 M" interface. It was this fraction #4 that contained the NPCs and was referred to as the highly enriched NPC fraction. Fraction #5 was the final 1 ml collected after vortexing to resuspend any pellet. This final gradient, though reproducible, also had the greatest tendency for variability and so great care was needed during its preparation and running.

For ion exchange chromatography and HPLC analysis, the proteins in fraction #4 or in the enriched nuclei were precipitated for 1 h with methanol (90% final concentration) at −20°C and resuspended in 10 mM Na-MES, pH 6.5, 100 mM DTT, 1.0% SDS. They were then diluted with 9 vol of 20 mM Na-MES, pH 6.5, 7 M urea, 1.0% Triton X-100 and batch incubated for 1 h at room temperature with S-sepharose resin (Pharmacia, Uppsala, Sweden) preequilibrated with column buffer (20 mM Na-MES, pH 6.5, 7 M urea, 1.0% Triton X-100, 0.1% SDS, 1 mM DTT). Unbound proteins were washed out of the resin with column buffer. Bound proteins were eluted with 1 M NaCl in column buffer. The two fractions were further separated by reverse phase HPLC, essentially as described (Pain et al., 1990; Wozniak, R., personal communication).

Gel Electrophoresis and Immunoblotting

Protein samples for SDS-PAGE (Laemmli, 1970) were either diluted directly with 0.5 vol of 3× sample buffer, or were concentrated by ultracentrifugation or by precipitation for 1 h with methanol (90% final concentration) at −20°C or TCA at 0°C, before resuspension in sample buffer. The samples were then incubated at 90°C for 10 min. All the gels presented here contained a 5–16% acrylamide gradient, and high and low molecular mass standards were used (BioRad Labs., Hercules, CA). Proteins were visualized after electrophoresis by staining with Coomassie brilliant blue, by silver staining, or by a combination of the two.

Immunoblots were prepared essentially as described in Towbin et al. (1979). They were then stained using the appropriate primary antibody as described in Wente et al. (1992). The only exception was with the monoclonal antibody MAb306, in which the Tween-20 was omitted from the blot buffer for all the incubations and washes. The blots were either exposed at −70°C on preflashed medical X-ray film or, in the case of quantitative immunoblotting for estimations of isolated NPC yields, the immunoblots obtained with MAb350 and MAb192 were exposed on a phosphor screen and the signals from NUP63 and NUP49 quantified using a PhosphorImager with ImageQuant software on an IBM PC (Molecular Dynamics, Inc., Sunnyvale, CA). To reduce variations and nonlinearities due to various immunoblotting artifacts (for review see Harlow and Lane, 1988), the signal intensities were then combined to obtain an overall yield.

Electron Microscopy and Image Processing

For negative stain electron microscopy, 15 μl aliquots of the sample were diluted with 15 μl of bt-DMSO buffer and centrifuged onto the surface of a glow discharged carbon-formvar 300 mesh copper grid at 1,800 *g* for 1 h at 4°C. The grid was then washed with bt-DMSO, and fixed with 3.7% formaldehyde, 0.5% glutaraldehyde in bt-DMSO for 20 min at 25°C. After washing with bt-DMSO, the grids were negatively stained with either 4% uranyl acetate or 2% potassium phosphotungstate (pH 7). Magnifications were calibrated using uniform latex microspheres of defined diameter (Duke Scientific Corp., Palo Alto, CA). Pairs of micrographs taken at 0° and 60° were made with a manually adjusted goniometer stage. Estimates of the thickness of NPCs (x) were made from measuring the NPC diameter parallel to the direction of tilt at 0° (D1) and at 60° (D2) from the formula:

$$x = \frac{1.4\{D1 - [D2 \cos 60°]\}}{\sin 60°}$$

The adjustment factor of 1.4 is an approximate compensation for z-axis compression in negative stain (Hinshaw et al., 1992).

For the image analysis, seven micrographs of fields of uranyl acetate negatively stained isolated yeast NPCs were scanned with a modified Joyce-

Loebl flatbed densitometer. The resulting image arrays were compressed a factor of three for display and particle selection. In all, 75 NPCs were chosen for further analysis based on the preservation of particle circularity and the appearance of subunit morphology. As the particle symmetry was not known a priori, the analyses were conducted as follows. Each particle was used as a reference in two complete alignment passes which encompassed rotational, translational, and flip/flop analyses using SPIDER (Frank et al., 1981; Akey, 1989). An average was then computed with and without enforced eightfold symmetry for each reference particle. Overall, eight particles were discarded as not aligning consistently. Therefore 67 particles were used for each average.

Samples for thin section electron microscopy were fixed in 1.25% glutaraldehyde, 0.2% tannic acid for 30 min at 25°C in their original buffer (usually sucrose-bt), and then for 16 h at 4°C in the same fixative buffered with 0.05 M potassium phosphate pH 7.0. After postfixation in 1% osmium tetroxide the samples were dehydrated with graded ethanol and embedded in Epon. Sections were stained with uranyl acetate and lead citrate. Magnifications were controlled for by measurements from structures of known dimensions (microtubules and SPBs).

All samples were viewed with a JEOL100CX electron microscope at 80 kV and photographed with Kodak electron microscope film.

Estimation of the Sedimentation Coefficient, Diffusion Coefficient, and Molecular Mass of the NPC

Enriched and highly enriched NPC fractions suitable for the following measurements was made as normal, except that the Triton X-100 and the Tween-20 added to the gradients (above) was replaced with octyl glucoside (Calbiochem Corp., La Jolla, CA) at the same concentrations. Under those conditions octyl glucoside would not form micelles, which might otherwise have interfered with the various measurements below. Yeast ribosomes prepared from yeast spheroplast homogenate (gift of C. Strambio de Castillia) were measured in parallel with the NPCs.

The sedimentation coefficients of both the NPCs and ribosomes were determined essentially as described by Griffith (1986). The enriched NPC fraction was dialyzed overnight at 4°C into bt-DMSO, 0.1% Triton X-100, 1:1,000 solution P, and both this and the ribosome standard were separately overlayered onto Beckman SW41 centrifuge tubes containing 11 ml linear gradients of 10–40% sucrose, 10 mM bisTris-Cl, pH 6.50, 0.3 mM $MgCl_2$, 0.5 mM K-acetate, 0.01% octyl glucoside, 1:1,000 solution P, and then centrifuged at 202,000 g_{av} and 5°C for varying times. The gradients were unloaded manually from the top and collected as 15 equal fractions of 733 μl. The linearity of all the gradients (an important assumption for the validity of the calculations) was confirmed after centrifugation by refractometric measurement of the sucrose concentrations of the collected fractions. The protein composition of the fractions was analyzed by SDS-PAGE and laser densitometry to determine quantitatively the peak fraction in each case. Negative stain EM was also performed on the fractions from one of the NPC gradients. Knowing the time and speed of the run and the sucrose concentration of the peak fraction, the time integral tables of both McEwen (1967) and Griffith (1986) could be used to calculate s-values.

The diffusion coefficients of the NPCs and ribosomes were measured using a Biotage dp801 molecular size detector, with software supplied by the manufacturers run on a Texas Instruments Travelmate 2000 PC. Both the NPC sample and ribosome standards were usually diluted 1:50 in 10 mM bisTris-Cl, pH 6.50, 0.1 mM $MgCl_2$, 0.35 mM KCl.

The density of NPCs was estimated by density sedimentation of the highly enriched NPC fraction and the ribosomes over linear 0.6 ml gradients of 1.75–2.50 M sucrose-bt, 0.01% octyl glucoside, 1:1,000 solution P at 237,000 g_{av} for 27 h at 20°C in a Beckman SW55Ti rotor. The resultant fractions were analyzed by refractometry and SDS-PAGE.

The molecular masses (M) were calculated from the sedimentation (s) and diffusion (D) coefficients using the formula:

$$M = \frac{sRT}{D(1 - \bar{\nu}\rho)}$$

(R = gas constant, 8.314×10^3 J kmol^{-1} K^{-1}; T = temperature, 293 K; ρ = density of water (293 K), 1.000 g cm^{-3}. The values used for the partial specific volumes ($\bar{\nu}$) of NPCs and ribosomes are taken as the inverse of their densities, which are given with explanations in the Results; Eason, 1984; Cantor and Schimmel, 1980). Error values for s and D are given as one standard deviation from the mean. An "error interval" of M_{min} to M_{max}, within which the best estimate value of M falls, was generated by finding the extreme values for M calculated using values for s and D plus or minus (as appropriate) the standard errors of their means, and the maximum and minimum possible values for the density.

Protein Assays

Protein concentrations were measured by the modified Bradford assay (Bradford, 1976) of either BioRad or of Pierce (Rockford, IL) ("Coomassie Plus"), using BSA as a standard. The relative amount of protein in various gradient fractions was measured from Coomassie blue-stained SDS polyacrylamide gels using a Pharmacia LKB Biotechnology Inc. (Piscataway, NJ) Bromma 2202 Ultroscan Laser Densitometer with a 2220 Recording Integrator.

Results

Comments on the Enrichment Procedure

It was noticed during the development of an enrichment procedure for yeast spindle pole bodies (SPBs; Rout and Kilmartin, 1990) that certain discrete particles were released from yeast nuclei upon nuclear lysis. Preliminary experiments supported the idea that the particles were indeed derived from yeast NPCs, as they contained a substantial portion of the original NPC components and had a comparable size and morphology to native NPCs (see also below). Although the exact degree of preservation of morphology and composition of these particles as compared with native NPCs has yet to be determined, they were for convenience termed NPCs and a method was developed to enrich for them as much as possible. Several criteria required for a large scale NPC enrichment procedure were already met by the existent SPB fractionation method (Rout and Kilmartin, 1990). First, yeast nuclei provide an excellent starting material for the production of NPCs. They can be made on a large scale and in high yield, and have the highest NPC:nuclear volume ratio of any eukaryote studied (Maul, 1977), potentially minimizing the amount of nuclear-derived contaminants. Yeast also have a closed mitosis, so that all cells presumably contain fully assembled NPCs (Byers, 1981). Second, both nuclear lysis and dispersal of the nuclear membranes were efficient and complete, separating SPBs and NPCs from potentially contaminating material (nuclear envelope, putative lamina, and chromatin) (Rout and Kilmartin, 1990). Third, after the nuclear lysate was separated over a step sucrose velocity gradient, the majority of the NPCs were recovered from a single fraction, suggesting that they were discrete and relatively homogeneous in size (Rout and Kilmartin, 1990). This fraction, recovered from the S/1.75 M interface of step sucrose gradient II and termed the crude NPC fraction, served as a basis for further enrichment as summarized in Fig. 1.

During the development of the enrichment procedure negative stain EM was used routinely, both as a semiquantitative assay for the presence of NPCs in fractions, and as a qualitative assay for the preservation of NPC morphology. This was complemented by SDS-PAGE and immunoblotting, to assay for the retention of known NPC proteins that were used as markers during enrichment. Both assays also monitored the amount of contaminating material present; as the crude NPC fraction was obtained from yeast nuclei, its major contaminants were derived from chromatin and nucleoli, as evidenced by the presence of histones and NOP1 (see below). By EM this material was heterogeneous, often aggregated, and entangled to varying degrees with the NPCs. DNase had already been used to disperse the nuclear chro-

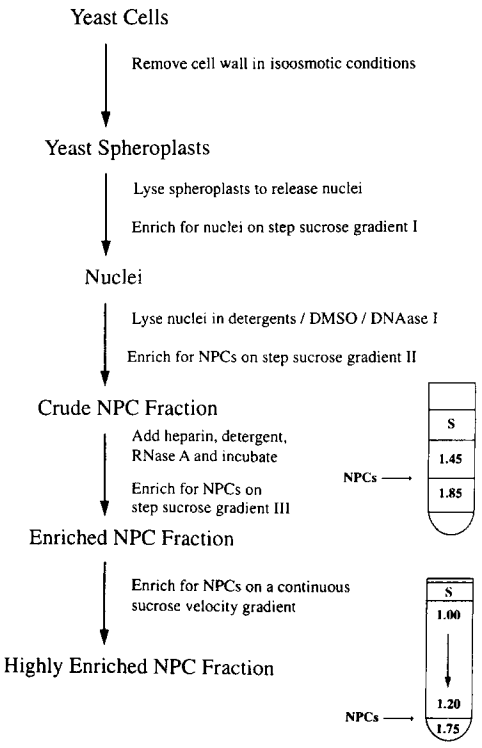

Figure 1. Flow diagram of the enrichment procedure.

matin, and additional exposure to this enzyme had no effect. Heparin has been used as an alternative to DNase in the solubilization of chromatin (Bornens and Courvalin, 1978) and it was found that low concentrations of this dispersed much of the contaminating material into particles considerably smaller than the isolated NPCs, without causing detectable alterations to the structure or composition of the NPCs themselves; however higher concentrations damaged the NPCs. The detergent sodium taurodeoxycholate, although having little effect on its own, was included as it seemed to act in synergy with the heparin to lower the effective concentration of the latter, thereby buffering the NPCs against its damaging effects. RNase was also included at this step but in fact its omission made little difference. Otherwise the buffer conditions required to preserve NPCs during the enrichment were similar to those used previously for stabilizing SPBs (Rout and Kilmartin, 1990).

The difference in size between NPCs and contaminating particles resulting from the heparin/sodium taurodeoxycholate treatment allowed them to be segregated from each other using velocity sedimentation gradients. A simple step gradient separated the isolated NPCs from most of the contaminants (step sucrose gradient III, Fig. 1). The resultant enriched NPC fraction was then graded by size on a continuous gradient (Fig. 1). EM revealed that most of the small particulate contaminants remained near the top of the gradient while the larger NPCs and occasional contaminating aggregates were found near the bottom. A basal cushion of higher density sucrose prevented the NPCs from pelleting while concentrating the resultant highly enriched NPC fraction. Two main problems were encountered during the development of these gradients. The first, aggregation of the isolated NPCs, was alleviated by the addition of nonionic detergents to solutions. This may reflect the presence of hydrophobic sites around the circumference of the NPCs, where they bind to the nuclear membranes. The second, apparent pressure-induced dissociation of the NPCs during centrifugation, was minimized by reducing the centrifugation speed, and by using gradient media containing DMSO and higher concentrations of sucrose. Samples of the highly enriched NPC fraction were centrifuged onto a highly charged electron microscope grid. The velocity gradients used in its preparation meant that only relatively large particles could be present at this stage, such that most should have sedimented onto the surface of the grid under these conditions. Examination of 550 particles in typical micrographs of the highly enriched fraction showed that ~90% resembled NPCs (Fig. 2).

Protein Composition of the NPC Fractions

The behavior of various known NPC and non-NPC proteins was followed throughout the enrichment procedure by SDS-PAGE and immunoblotting. Fig. 3 *A* shows a Coomassie blue-stained SDS-polyacrylamide gel on which were loaded protein samples from all the fractions collected during the enrichment procedure. Those fractions containing most of the NPCs as determined by EM as well as immunoblotting (see below) are indicated at the top of the gel.

Several bands served as markers, representing known non-NPC proteins from different regions of the cell that might contaminate the NPC fractions. These were recognized either by their characteristic Coomassie staining patterns or by monospecific antibodies on immunoblots. Thus by Coomassie staining, nuclear proteins are represented by the four histones (Fig. 3 *A*, lane *7*, positions marked with dots; Thomas and Furber, 1976; Nelson et al., 1977). A band at around 50 kD was believed to be a cytoplasmic protein, and was found to be a persistent contaminant of yeast fractionation procedures (Fig. 3 *A*, marked with an arrowhead; Kilmartin, J. V., personal communication; Rout and Kilmartin, 1990). Immunoblotting was used to detect the 110-kD SPB protein (associated with the nuclear envelope; Fig. 3 *B*), tubulin (in both the nucleus and cytoplasm; Fig. 3 *C*) and the nucleolar protein NOP1 (Fig. 3 *D*; Aris and Blobel, 1988; Kilmartin and Adams, 1984; Rout and Kilmartin, 1990). None of these proteins coenriched absolutely with the NPCs, although as expected most of the tubulin, the histones, the SPB protein, and NOP1 followed them as far as the enriched nuclear fraction. However, little of these proteins could be found in the final highly enriched NPC fraction. The loss of specific non-NPC components during the enrichment procedure was associated with a huge decrease in the total amount of protein in the NPC-containing fractions (Fig. 3 *A*; Table I). By contrast, a large number of unidentified Coomassie-staining bands coenriched absolutely with the NPCs. This was emphasized by silver staining of the final five gradient fractions (Fig. 3 *A*, *right*). Three such high molecular mass bands were particularly noticeable (Fig. 3 *A*, marked with *arrows*), and could be seen to follow the NPCs in the last two gradients.

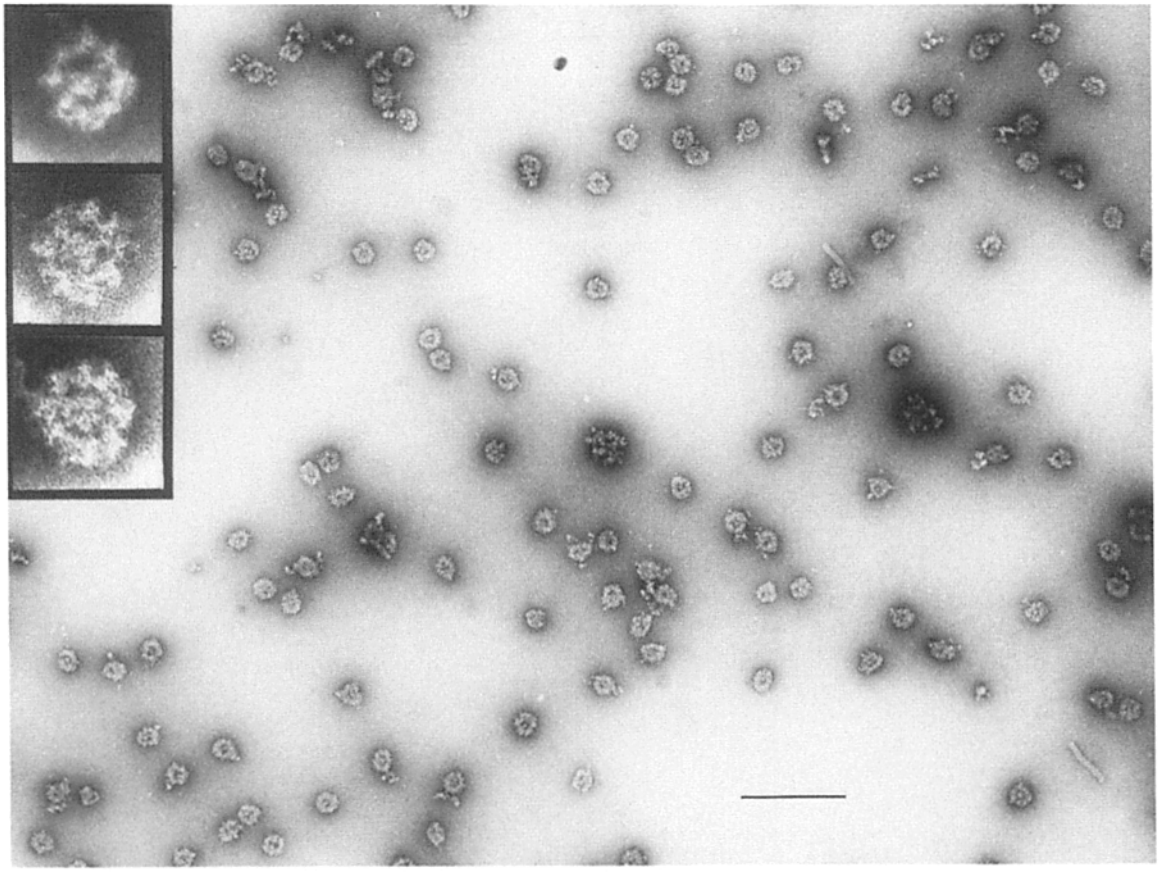

Figure 2. (*Main figure*) Electron micrograph of the negatively stained highly enriched NPC fraction showing a field of isolated NPCs and occasional contaminants; stained with uranyl acetate. Bar, 0.5 μm. (*Inset*) Three examples of negatively stained isolated NPCs in this fraction showing their overall morphology of eight spokes surrounding a central plug. Bar on main figure is ~90 nm long at the scale of the inset.

Equal protein loadings from both the highly enriched NPC fraction and the enriched nuclei fraction were separated by ion exchange chromatography and reverse phase HPLC in an attempt to distinguish between specifically coenriching proteins and contaminants, especially in the more crowded lower molecular mass regions. The two separation profiles obtained were very different (Fig. 4). A more detailed comparison revealed that the two fractions shared at least 40 bands of the same apparent molecular mass and column separation characteristics, which probably represent noncoenriching contaminants of the NPC fraction. Amongst these are the histones (indicated with an asterisk in Fig. 4), which are prominent proteins of the nuclear fraction but are present in relatively minor amounts in the NPC fraction. Roughly 40 relatively major bands and at least a further 40 minor bands were highly enriched in the NPC fraction, and were therefore candidate NPC proteins.

Immunological Analysis of the NPC Fractions

Having shown that non-NPC proteins did not coenrich with the isolated NPCs it was necessary to determine the degree of cofractionation of known NPC components. A panel of monoclonal antibodies raised against rat NPC-containing fractions have been previously shown to contain members that recognize yeast NPC proteins. The NPC proteins so detected belong to related families of proteins that share one of two domains containing either numerous conserved nonapeptide or tetrapeptide repeats (Davis and Blobel, 1986, 1987; Aris and Blobel, 1989; Davis and Fink, 1990; Wente et al., 1992; Loeb et al., 1993). From this panel four monoclonal antibodies, MAb350, MAb414, MAb192, and MAb306, were chosen for further study. They have been shown to recognize six such previously described NPC proteins; NUP1 and NSP1 (Davis and Fink, 1990), NUP2 (Loeb et al., 1993), and NUP116, NUP100, and NUP49 (Wente et al., 1992). Two related proteins, provisionally termed NUP63 and NUP54, were also recognized and determined to be NPC proteins (Wente, S. R., personal communication). All the antibodies were found to give staining patterns characteristic of NPCs on both indirect immunofluorescence and immunoelectron microscopy of S. uvarum cells (data not shown).

Fractions from the enrichment procedure were separated by SDS-PAGE as in Fig. 3 and immunoblotted with the four monoclonal antibodies. The results are shown in Fig. 5, where the fractions containing most of the NPCs as indicated by the EM assay are marked with a star above their respective lanes. All blots were overexposed to reveal the fainter bands. The simplest pattern obtained was that from MAb306. It recognized three major bands, one around 120 kD and a doublet at ≈100 kD (somewhat obscured due to the overexposure). The 120-kD band and the upper of the 100-

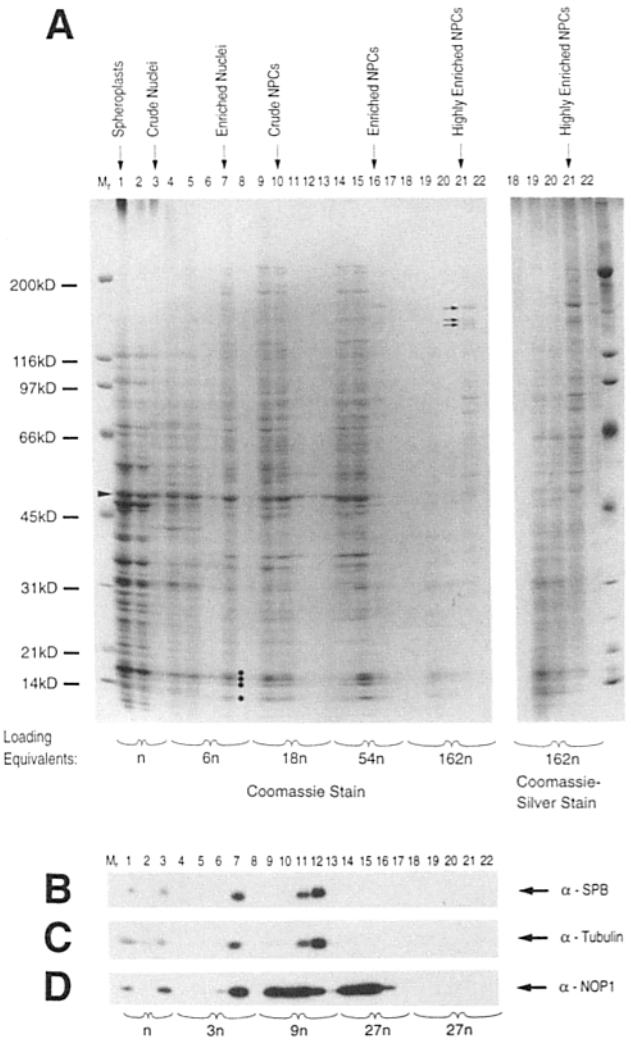

Figure 3. The enrichment procedure as monitored by SDS-PAGE and immunoblot analysis, showing the loss of many non-NPC proteins and coenrichment of a distinctive subset of bands with the NPC-containing fractions. (Lane *1*, *arrow*) Whole spheroplast lysate; (lanes *2* and *3*, *arrow*), postnuclear supernatant and crude nuclear pellet, respectively. (lanes *4–8*) Fractions from sucrose gradient centrifugation of the crude nuclear pellet (Fig. 1, step sucrose gradient I), from which is recovered the enriched nuclear fraction (lane *7*, *arrow*; Rout and Kilmartin, 1990). (lanes *9–13*) Sucrose gradient II (Fig. 1), separating the total nuclear lysate into amongst others a crude NPC fraction (lane *10*, *arrow*) and a crude SPB fraction (lane *12*; Rout and Kilmartin, 1990). (lanes *14–17*) Fractions collected from centrifugation of the crude NPC fraction over the step sucrose gradient III (Fig. 1). (lane *14*) the S fraction; (lane *15*) the S/1.45 fraction; (lane *16*, *arrow*) the 1.45/1.85 fraction, termed the enriched NPC fraction; (lane *17*) the 1.85/2.5 fraction. (lanes *18–22*) Fractions #1 to #5, respectively, collected from the continuous velocity gradient centrifugation of the enriched NPC fraction (Fig. 1). (lane *21*, *arrow*) Fraction #4, the final highly enriched NPC fraction. For fraction nomenclature see Materials and Methods. Figures along the bottom of the gel indicate the number of cell equivalents (*loading equivalents*) required to produce the amount of protein loaded in each lane for the fractions from each gradient, with reference to an arbitrary value (*n*) for the starting number of cells. It was necessary to increase the loading equivalents for the more enriched NPC fractions in order to be able to visualize their proteins. Molecular mass standards (M_r) are shown to the left of the gels.

Table I. Estimated Yield of NPC Protein during the Enrichment Procedure

Fraction	Total protein (*mg*)	NPC protein (*mg*)*	Fold enrichment	Yield (%)
Spheroplasts	4200	6.2	–	100
Crude nuclei	1100	4.8	3	78
Enriched nuclei	260	3.9	10	62
Crude NPCs	50	3.1	40	49
Enriched NPCs	9.0	2.8	213	46
Highly enriched NPCs	3.1	2.8	607	45

* Based on an estimated NPC M_r of 66 MD, 189 NPCs/nucleus, 3×10^{11} spheroplasts; and on the yield (%) estimates from the quantitative immunoblotting data (see text).

kD doublet coenriched entirely with the NPC-containing fractions. Both of these antigens have been identified as the NPC proteins NUP1 and NSP1, respectively (Davis and Fink, 1990; Nehrbass et al., 1990). The coenrichment of NSP1 with the isolated NPCs was confirmed by immunoblotting with a polyclonal monospecific anti-NSP1 antibody (a gift of U. Nehrbass and E. Hurt; data not shown), which also indicated that the minor bands below 100 kD were probably proteolytic degradation products. The identity of the lower band of the doublet has also been recently established as being another NPC protein, NUP2 (Loeb et al., 1993). However NUP2 did not coenrich with the isolated NPCs in this procedure, separating from them after the crude NPC fraction (Fig. 5, MAb306; compare lane *10* and lane *16*, with NUP2 present or absent, respectively).

MAb192 gave a more elaborate pattern as it cross-reacted with two low molecular mass bands at ~35 and 12 kD, both of which remained in the cytoplasmic supernatant at the first stage of nuclear enrichment (Rozijn and Tonino, 1964), and also recognized five major antigens coenriching with the NPCs (Fig. 5). These five bands represented the three NPC proteins NUP116, NUP100, and NUP49, as well as the two NPC proteins NUP63 and NUP54. Minor coenriching bands between NUP100 and NUP63 were probably proteolytic degradation products of NUP116 and NUP100 (Wente et al., 1992; Wente, S. R., personal communication).

The monoclonal antibodies MAb350 and MAb414 both

(*A*, *Left*) Coomassie blue-stained gel of all the fractions from the enrichment procedure. The fractions containing the majority of the NPCs in each gradient are indicated along the top of the gel (*arrows*). The non-coenriching histone bands (*dots*) and 50 kD cytoplasmic band (*arrowhead*) are indicated on the gel, as are the three prominent bands that coenrich with the NPCs (*arrows*). (*Right*) Coomassie/silver-stained gel of the five fractions from the final velocity gradient producing the highly enriched NPC fraction, showing many distinctive bands coenriching with the NPCs. (*B–D*) Immunoblot of an SDS polyacrylamide gel prepared in a similar manner to that in *A* and probed as described in Materials and Methods for known non-NPC proteins. (*B*) The 110-kD SPB protein, detected with the monoclonal antibody 3D2 (Rout and Kilmartin, 1990). (*C*) Yeast tubulin, detected with a polyclonal affinity purified rabbit anti-yeast tubulin (Rout and Kilmartin, 1990). (*D*) The yeast nucleolar protein NOP1, detected with the monoclonal antibody D77 (Aris and Blobel, 1988). Lane number and loading equivalent nomenclature is as described above.

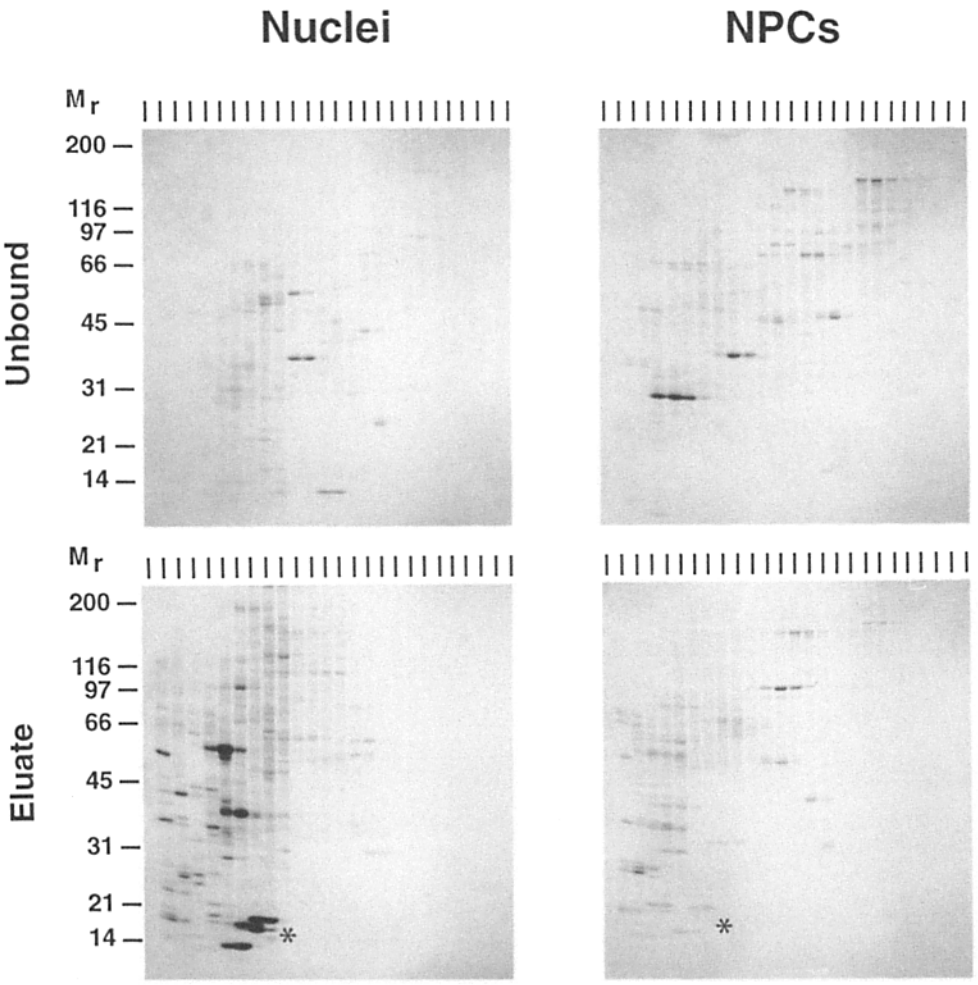

Figure 4. Ion exchange and HPLC chromatography showing equal protein loadings of samples from the enriched nuclei fraction (*Nuclei*) and highly enriched NPC fraction (*NPCs*), to show the number of different polypeptides they contain and the proteins that coenrich with the highly enriched NPC fraction, which are 60-fold enriched over the nuclei fraction (Table I). Four parallel gels were run by normal SDS-PAGE and stained with Coomassie blue. The approximate M_r of proteins as estimated from molecular mass standards are shown down the left side. Each gel shows the proteins in the unbound or eluate fraction, resulting from ion exchange chromatography of either the nuclei or NPC sample, and further separated by reverse phase HPLC into 26 fractions, loaded left to right on the gel in the order they were collected according to increasing hydrophobicity. The position of each HPLC fraction is indicated above each gel by a vertical line (see Materials and Methods; Wozniak, R., personal communication). An asterisk indicates the position of the bands believed to be the four histones, that are amongst the bands common to both the nuclei and NPC samples.

gave similar and complex staining patterns. They cross-reacted strongly with several antigens that remained in the cytoplasmic supernatant, including bands at ~50 kD, one of which may have been the previously described non-nuclear 53-kD polypeptide (Davis and Fink, 1990), and a 25-kD band. Two antigens at ~95 and 110 kD coenriched with the NPCs as far as the crude NPC fraction, but were subsequently lost. The lower of these was likely to be the NUP2 protein described above, as this can be recognized by MAb350 and MAb414 as well as MAb306 (Loeb et al., 1993). The other antigen may have been another, as yet unidentified, NPC protein because of its similar reactivity to and cofractionation with NUP2. Six remaining bands coenriched completely with the NPCs. The faint band at ~120 kD and the 100-kD band were due in part to NUP1 and NSP1, respectively (Davis and Fink, 1990). The upper band was virtually undetectable in the first few fractions with MAb414 (Fig. 5, lanes *1–10*). The next three antigens down were again most likely to be NUP63, NUP54, and NUP49, as they are known to cross-react with both of the antibodies (Davis and Fink, 1990; Wente et al., 1992; Wente, S. R., personal communication). The identity of the minor band at ~45 kD was not determined. It is probable that MAb350 and MAb414 also recognized NUP116 and NUP100 on the cell fractionation immunoblots as they recognize these proteins when expressed in *E. coli* (Wente, S. R., personal communication), and that the signals seen at the 120- and 100-kD positions were combinatorial. This has not yet been confirmed on immunoblots of the NPC fractions.

Thus the bands recognized by the antibodies fall into three categories. The first contained those antigens that were lost immediately to the cytoplasmic fraction. They may represent the fortuitous recognition by the antibodies of relatively abundant non-NPC proteins. For example, MAb350 reacted with the radiolabeled 31-kD carbonic anhydrase molecular mass standard (Fig. 5), which is most certainly not an NPC protein! Similar problems have been encountered with an independent panel of monoclonal antibodies against the rat homologues of these NPC proteins (Snow et al., 1987; te Heesen et al., 1991). The second category contained seven known yeast NPC proteins that coenriched absolutely with the NPCs, demonstrating that the particles being enriched for were indeed derived from yeast NPCs. The third category contained the two antigens lost from the NPC-contain-

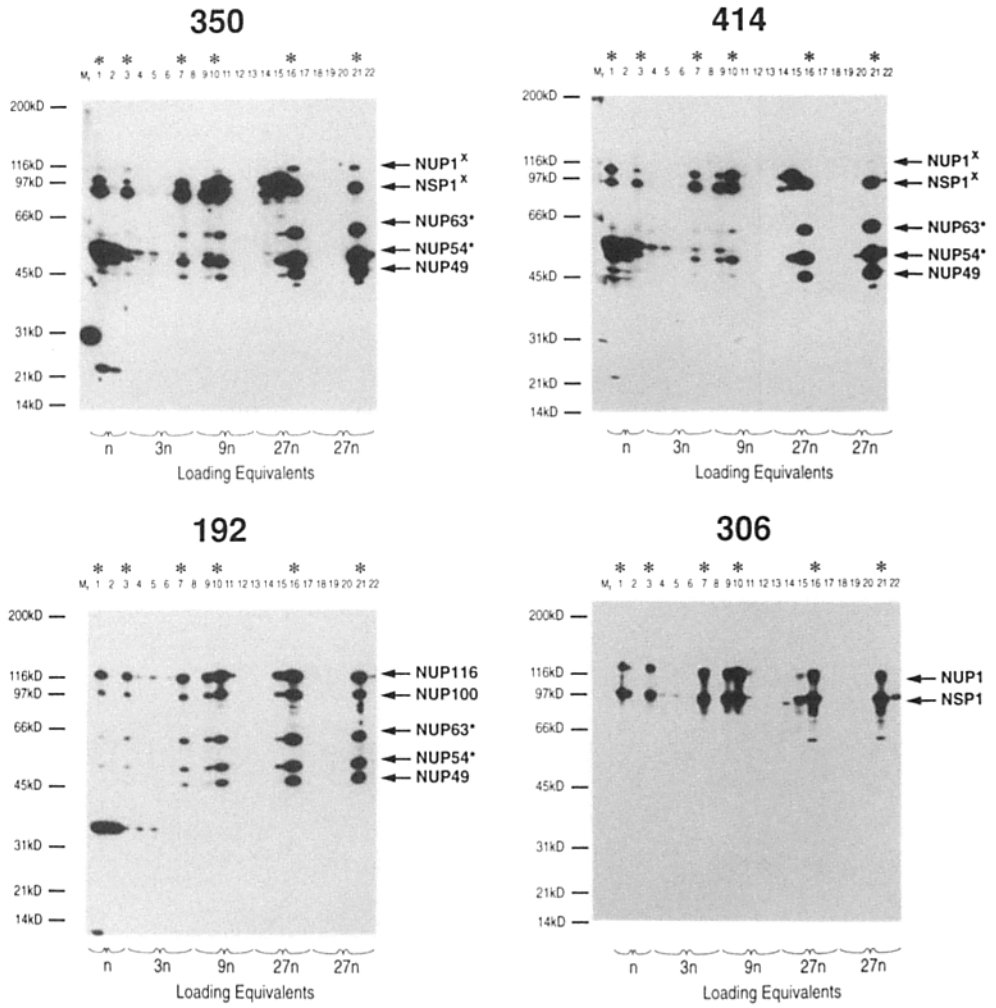

Figure 5. Known NPC proteins coenrich with the NPC-containing fractions. Immunoblots of four identical SDS-polyacrylamide gels prepared as described in Fig. 3 and probed with the monoclonal antibodies MAb350 (*350*), MAb414 (*414*), MAb192 (*192*), and MAb306 (*306*). Lane number and loading equivalent nomenclature are also as described in Fig. 3. The NPC-containing fractions are indicated along the top of the gel (*asterisks*), and molecular mass standards (M_r) are shown to the left of the gels. The approximate banding positions of the known yeast NPC proteins recognized by these antibodies are indicated to the right side of each immunoblot; those marked with a star are still being characterized. *NUP1^x*, probable combinatorial signal from NUP1 and NUP116; *NSP1^x*, probable combinatorial signal from NSP1 and NUP100.

ing fractions part way through the enrichment procedure. One of these is certainly an NPC protein (NUP2), emphasizing that the NPCs in the final highly enriched fraction are not completely intact. The immunoblots have also been probed with WGA. No bands coenriching with the NPCs were specifically recognized by this lectin.

The percentage yield for the isolated NPCs was calculated for each gradient based on the NPC proteins NUP63 and NUP49 (Table I), from measurements of their relative signal intensities on both the MAb192 and MAb350 immunoblots (see Materials and Methods). The total amounts of protein in each fraction were estimated as described in Materials and Methods, and inaccuracies in these measurements were reduced by using several different quantitation methods in parallel. These data were used with the NPC molecular mass estimates (see below) and an average of 189 NPCs per yeast cell (from serial thin sections of nuclei; data not shown) to calculate a balance sheet for the NPC enrichment procedure, presented in Table I. From this it can be seen that the NPCs were recovered as an ~90% pure fraction, though in fact this is more likely to be in the range of 75–90% (see below), with a 45% yield and more than 600-fold enriched over spheroplasts.

Electron Microscopy of the NPC Fractions

A detailed investigation of yeast NPC ultrastructure has been frustrated for a number of reasons (Nehrbass and Hurt, 1992), but chief amongst these is a shortage of unobscured isolates from yeast similar to those used in the study of vertebrate NPCs. Thus the morphology of the NPCs was examined at various stages in the enrichment procedure (during which varying degrees of obscuring material is removed) in the hope that, despite possible losses and distortions, details of yeast NPC ultrastructure might be elucidated. The enriched nuclei and highly enriched NPC fractions proved particularly suitable for such an investigation. Data obtained from both fractions are united here to give an overall picture of yeast NPC morphology.

It was clear that at a superficial level, yeast NPCs strongly resembled those in other eukaryotes, each being a short cylinder containing a central plug surrounded by a coaxial annulus of octagonal symmetry (the eight spokes; Fig. 2, *inset*; Fig. 6 *D*). This octagonal symmetry was confirmed by unbiased (i.e., in which no symmetry was assumed a priori) computer processing of electron micrographs from 75 negatively stained isolated NPCs (analysis performed by C. W. Akey; Frank et al., 1981; Akey, 1989; Akey, 1990; Akey and Radermacher, 1993). The results are shown in Fig. 6; examples for three particles are shown in the figure. The first column contains the unprocessed particle image used as the reference. The second column contains the average obtained by alignment of 67 particles after using the particle to the left as a reference (eight particles were discarded from the

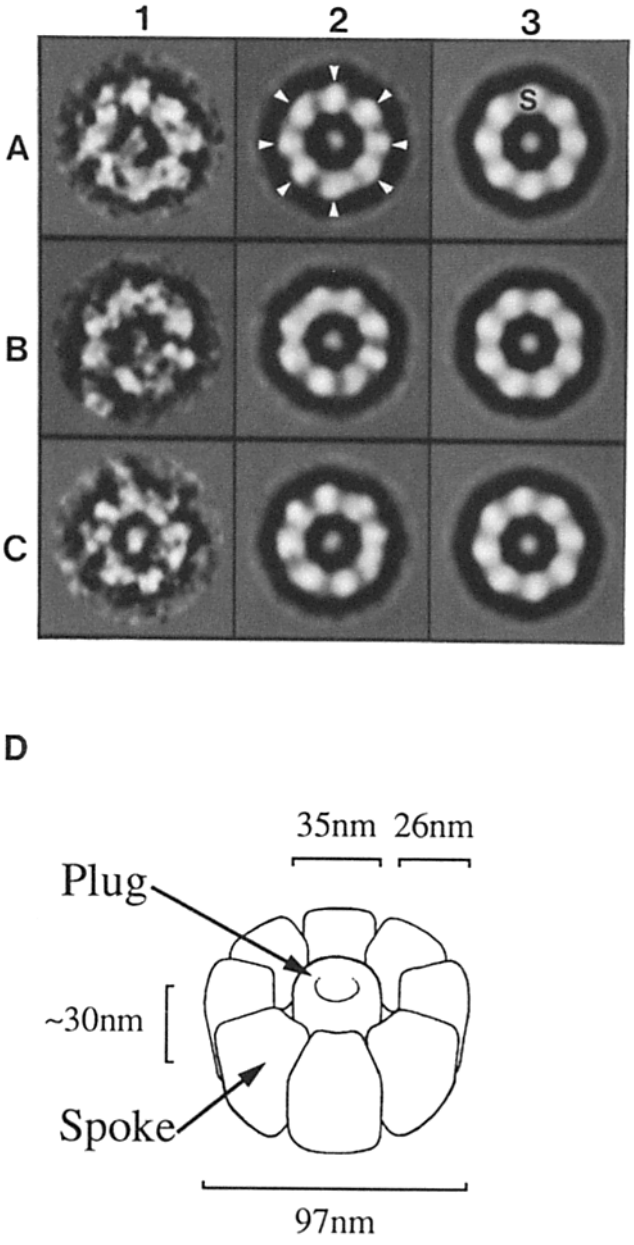

Figure 6. Image analysis of the isolated NPCs (data kindly provided by C. W. Akey). (*1*) Column containing the unprocessed NPC image used as a reference. (*2*) Column containing the average of 67 NPCs after using the particle to the left as a reference. (*3*) Column containing the eightfold average for each dataset. Examples for three reference NPCs (*A*, *B*, and *C*) are shown in the figure. (*D*) Diagrammatic interpretation of the ultrastructural features and measured dimensions of the negatively stained isolated NPCs.

dataset by the computer as being unalignable, either because they were damaged NPCs or contaminants). The third column contains the eightfold average for each dataset. This analysis provided four striking observations. First, both the best individual images (Fig. 2, *insets*; Fig. 6, column *1*) and all of the 67 averaged images (Fig. 6, column *2*) have clear octagonal symmetry. This symmetry is manifested as an angular spacing of 45° between adjacent spokes. Second, after enforcing eightfold symmetry on the final aligned averages calculated from each single particle, the final averaged maps

Table II. Dimensions of Yeast NPCs

	In isolated NPCs	In nuclei
Plug diameter	35 ± 4 nm (200)	29 ± 3 nm (6)
Spoke radial length	26 ± 4 nm (200)	26 ± 2 nm (5)
NPC diameter	97 ± 5 nm (200)	97 ± 5 nm (10)
NPC thickness	27 ± 4 nm (200)	32 ± 6 nm (100)
Basket height	– (–)	50 ± 8 nm (10)

Measurements were made on electron micrographs of NPCs in the highly enriched NPC fraction negatively stained with phosphotungstate (In isolated NPCs), or on thin section electron micrographs of NPCs in the enriched nuclei fraction (In nuclei). Each mean value is given with its standard deviation. Figures in brackets are the number of measurements made to obtain each mean value. A minus sign indicates that the measurement could not be made.

are identical (with the exception of differing rotational orientations). This indicates that the entire dataset of particles aligned in a rotational manner consistent with eightfold symmetry, regardless of the reference particle used in the computation. Third, in many individual examples and in the aligned averages each spoke was subdivided into an inner and outer spoke domain of approximately equal sizes by a faint darker line (Fig. 6). Xenopus NPC spokes are similarly subdivided, although they display an extra domain (Unwin and Milligan, 1982; Akey, 1989; Reichelt et al., 1990; Hinshaw et al., 1992; Akey and Radermacher, 1993). Fourth, the apparent outer diameter of the spoke annulus is ~100 nm in projection, 20 nm smaller than the vertebrate NPC; thus the spoke in the isolated NPCs, at ~28 nm, is only two-thirds the length of the Xenopus NPC spoke. However, the inner diameter of the spoke annulus is conserved, measuring roughly 44 nm (Unwin and Milligan, 1982; Akey, 1989; Reichelt et al., 1990; Hinshaw et al., 1992; Akey and Radermacher, 1993). The presence of the plug was also retained in the averages, but these analysis techniques did not preserve its morphology. The measurements from the aligned averages were in excellent agreement with those made from 200 individual isolated NPCs. More than 90% of the isolated NPCs examined also contained plugs, of a diameter comparable to that seen in vertebrates (Table II). The length of the isolated NPC along its cylindrical axis was estimated at ~30 nm by trigonometric measurements of tilt pair micrographs (see Materials and Methods; Table II), although such images showed no clear evidence for the presence of cytoplasmic or nuclear rings on the isolated NPCs.

The possibility of the specific loss of material from the isolated NPCs led to similar studies being made on the NPCs in thin section electron micrographs of yeast nuclei, a fraction more comparable to those used for the measurements of Xenopus NPCs (Unwin and Milligan, 1982; Akey, 1989; Reichelt et al., 1990; Hinshaw et al., 1992; Akey and Radermacher, 1993). Although the detailed NPC morphology was more difficult to discern in the nuclei, all the NPCs examined in tangential sections contained a plug surrounded by a densely staining annulus (Fig. 7 *A*). Detailed examination of transverse thin sections of NPCs in yeast nuclei did not show clear examples of the cytoplasmic and nuclear rings found in Xenopus NPCs (Fig. 7, *B* and *C*), and measurements from such sections yielded an estimate of ~30 nm for the NPC thickness (Table II), similar to that for the isolated NPCs but less than half the 70–80 nm estimated for the Xenopus NPC (Hinshaw et al., 1992; Akey and Radermacher, 1993). Thus it is not clear whether the isolated NPCs retained such rings,

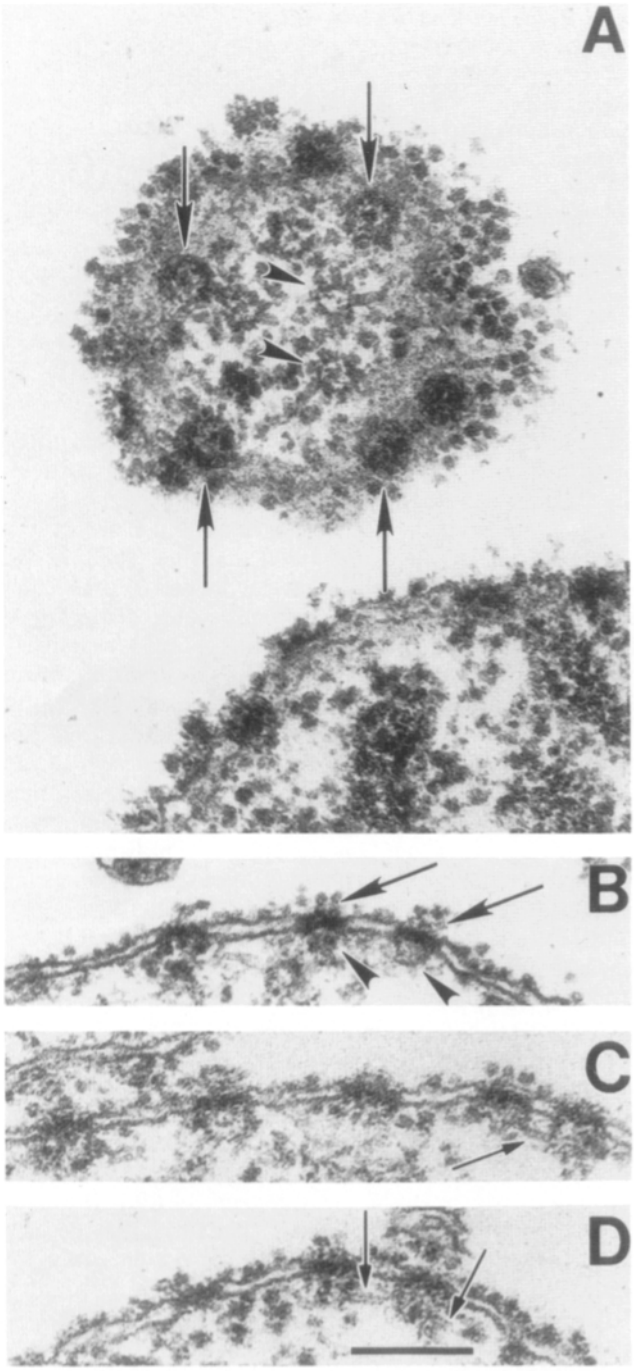

Figure 7. Thin section electron micrographs of pelleted yeast nuclei, illustrating ultrastructural features of the yeast NPCs. (*A*) Micrograph showing transverse section (*lower right*) and tangential section (*center*) of the nuclear envelope and peripheral chromatin. (*Arrows*) NPCs sectioned in the plane of the nuclear envelope showing their plugs and spoke rings. (*Arrowheads*) NPCs sectioned through a plane parallel to and just on the nuclear side of the nuclear envelope showing the NPC basket with tubules apparently radiating from a distal ring. (*B–D*) Transverse sections of the nuclear envelope and peripheral chromatin. (*B*) Arrowheads show the baskets associated with the nucleoplasmic side of NPCs and arrows show the diffuse material on their cytoplasmic side. (*C* and *D*) Arrows show the tubules between the baskets. Bar, 0.2 μm.

nor if they are present in yeast NPCs at all. Surprisingly, the measurements obtained from the NPCs within the context of the yeast nuclei were very similar to those obtained from the isolated NPCs (Table II), though they are in full agreement with the dimensions of NPCs as seen in preparations of yeast cells (Moor and Mühlethaler, 1963; Severs et al., 1976; Willison and Johnston, 1978; Byers, 1981).

There was little evidence for the extensive cytoplasmic filaments seen on Xenopus NPCs (Franke, 1974; Richardson et al., 1988; Ris, 1990, 1991; Jarnik and Aebi, 1991; Goldberg and Allen, 1992) although there was usually a 20–30-nm thick layer of disordered material associated with the cytoplasmic face of the yeast NPCs (Fig. 7 *B*, *arrows*). On the other hand filamentous structures projecting from the nuclear face of the yeast NPCs were often visible (Fig. 7 *B*, *arrowheads*). In transverse section the structures formed by the nucleoplasmic filaments were ~50 nm long (Fig. 7, *B–D*; Table II). Tangential sections cut through these structures suggested that eight such filaments projected from each NPC and were arranged octagonally in a circle, presumably such that a single filament originates from each spoke (Fig. 7 *A*, *arrowheads*). At the end distal to the NPC the adjacent filaments appeared to be fused into a ring. These structures thus resembled the baskets seen on the nucleoplasmic face of Xenopus NPCs, although the Xenopus basket can extend more than 100 nm into the nucleoplasm (Jarnik and Aebi, 1991). Curiously, it was also noticed that the putative distal basket rings in yeast seemed to be the attachment site for short tubular fibers, which radiated out parallel to the nuclear envelope and sometimes connected neighboring baskets (Fig. 7 *A*; Fig. 7, *C* and *D*, *arrows*). Fibers connecting the distal regions of baskets have been seen in Xenopus preparations (Ris, 1991; Jarnik and Aebi, 1991; Goldberg and Allen, 1992).

Mass Measurements of the Isolated NPCs

The estimation of the degree of enrichment of the highly enriched NPC fraction (Table I) first required the determination of the molecular mass of the isolated NPC; for this to be estimated, accurate values for the sedimentation coefficient, diffusion coefficient, and density of the NPC needed to be measured (Cantor and Schimmel, 1980; Eason, 1984). A preparation of 80 S yeast ribosomes was measured in parallel to provide an estimate of the accuracy of the values obtained for the yeast isolated NPCs. The sedimentation coefficient, mass, and density of the yeast ribosome were already known (Chao and Schachman, 1956; Chao, 1957).

As no sedimentation standards of suitable range were available, the sedimentation coefficients were estimated by centrifugation using time integral values for the particles, measured on isokinetic sucrose gradients (McEwen, 1967; Griffith, 1986). The position in the gradient of both the ribosomes and the NPCs was determined by SDS-PAGE. The position of the NPCs in the gradient was confirmed by negative stain EM. This also showed that they had neither disintegrated nor aggregated during the centrifuge run, which would have artifactually altered their sedimentation properties. This method gave a mean sedimentation coefficient of 310 S for the NPCs and 79 S for the ribosomal standards (Table III). The ribosomal figure was very close to the previ-

Table III. Physical Properties of Yeast NPCs

	Isolated NPCS	Ribosomes
Sedimentation coefficient ($s \times 10^{13}$ s)	310 (±39)	79 (±1)
Diffusion coefficient ($D \times 10^{13}$ m^2s^{-1})	54 (±4)	135 (±24)
M_r (megadaltons)	66 (56-73)	4.3 (4.1-4.4)

Mean sedimentation coefficient values are given, calculated from five measurements (NPCs) and two measurements (Ribosomes). Mean diffusion coefficient values are given, calculated from 68 measurements (NPCs) and 64 measurements (Ribosomes). Molecular mass values, and error values (in brackets), are calculated as described in Materials and Methods.

ously determined value of 80 S (Chao and Schachman, 1956).

The diffusion coefficients were measured with a Biotage dp801 molecular size detector (with S. Burley). The mean diffusion coefficients obtained are presented in Table III. Although the measurements from the NPC samples were fairly even, those from the ribosome standard samples were more widely scattered around their mean. The reasons for this were not known.

The density of yeast ribosomes has already been determined (1.5 g/ml; Chao and Schachman, 1956). Although it was impracticable to determine the absolute density of the NPCs, an approximate value was obtained by density gradient centrifugation of both the isolated NPCs and ribosomes on sucrose gradients. Most NPCs were found at densities between 1.24 and 1.27 g/ml. The ribosomes were found at densities above 1.3 g/ml (data not shown). Though they had not reached equilibrium, the slower sedimenting but higher density ribosomes overtook the NPCs by a wide margin. Thus it was considered likely that the NPCs had banded close to their equilibrium density, and that the true density of the isolated NPCs is probably around 1.27 g/ml, a figure often used for the average density of pure proteins (Rickwood, 1984). The possibility of their density being as high as 1.30 g/ml (a figure also used as typical of pure proteins; Griffith, 1986) was accounted for in the error calculations.

Clearly, an unknown amount of contaminant actually adhering to the isolated NPCs would increase their apparent mass. The material seen in or next to the plugs was unlikely, due to its small volume, to contribute much more than 5% to the NPC mass value. The amount associated with the surface of the NPC, and its contribution to the NPC mass, could not be estimated. However it was also considered unlikely to contribute much to the mass value, as it was not enough to obscure the morphological features observed in the isolated NPCs.

From these figures the molecular masses of the ribosomes and NPCs were estimated (Table III). It was not possible to calculate a standard deviation for the molecular mass estimate as it is derived from a ratio of variables, but an error interval was derived within which the best estimate of the molecular mass was likely to fall (Table III; see Materials and Methods). The calculated molecular mass for the ribosomes was 4.3 MD, reassuringly close to the value of 4.1 MD previously obtained for yeast ribosomes (Chao and Schachman, 1956). The molecular mass of the isolated yeast NPCs was estimated to be 66 MD. This is approximately half the mass measured for Xenopus oocyte NPCs (125 MD; Reichelt et al., 1990) but is consistent (at least in part) with the comparatively smaller dimensions of the yeast NPC as compared with those of Xenopus.

Purification of NPC Proteins

It became possible to draw some preliminary conclusions as to the composition of the isolated yeast NPCs. The density of the NPCs was clearly much less than that of ribosomes and close to the density of pure protein. Hence, if RNA is a constituent part of the NPCs as has been suggested (Scheer, 1972) then it is probably a fairly minor component. The NPC mass estimates (Table III) and immunoblot yield figures (Table I) predict that as much as 90% of the protein in the highly enriched fraction was from NPC components. Even the lowest NPC mass estimate (56 MD; Table III) predicts that 75% of the protein in the highly enriched fraction was from NPC components. When the protein composition of the highly enriched NPC fraction was investigated by column chromatography and SDS-PAGE (Figs. 3 and 4), over 80 of the roughly 120 polypeptides in the highly enriched NPC fraction specifically coenrich with the isolated NPCs. These figures are consistent with this fraction's purity estimated both qualitatively by electron microscopy (Fig. 2), and quantitatively by immunoblotting (Table I). It is possible that some of these polypeptides were derived from proteolysis of other proteins, although this would seem unlikely to be a major problem since only minor proteolysis of nucleoporins was seen on the immunoblots (Fig. 5, MAb306), even for proteins such as NSP1 which have been shown to be proteolytically sensitive (Hurt, 1988).

It should therefore be relatively straightforward to identify candidate NPC proteins in the highly enriched NPC fraction by comparison with a similar preparative scale purification of proteins from yeast nuclei; such NPC proteins would be strongly enriched in the highly enriched NPC fraction, much as they were in the analytical gels (Fig. 4). There ought to be little confusion of NPC proteins with contaminant proteins as the latter appeared to be in the minority in both numbers and quantity in the highly enriched NPC fraction. Thus it should be possible to make microgram quantities of each of the NPC proteins for the purposes of obtaining protein sequence data, to be used in the cloning of their corresponding genes. That this is indeed the case was shown first with NPC proteins that could be independently verified. After separation of the NPC fraction using HPLC and SDS-hydroxylapatite chromatography as described (Wozniak, R., G. Blobel, and Rout, M., unpublished data), immunoblotting with MAb192 identified NUP116, NUP100, and NUP49 as being present in single Coomassie-staining bands on SDS-PAGE of the chromatographic fractions (Wente, S., and R. Wozniak, personal communication). All the internal peptide sequences obtained from these bands were found within the predicted amino acid sequences derived from each of their corresponding genes, and indeed proved helpful during the identification of NUP49 (peptide sequence data provided by R. Wozniak; Wente et al., 1992; data not shown). This strongly suggests that each of the three bands contained only one species of protein, those being NUP116, NUP100, and NUP49, respectively. The method therefore seemed generally applicable to the characterization of NPC proteins in the highly enriched fraction and has since been used successfully in the isolation of genes encoding novel NPC proteins (Wozniak, R., G. Blobel, and M. Rout, unpublished data).

Discussion

This paper presents a method for the production of milligram quantities of highly enriched particles, referred to as isolated NPCs as they retained most of the assayable morphological and biochemical features found in NPCs in situ. The procedure has proven reproducible, and preliminary results have suggested that other *S. cerevisiae* strains may be successfully substituted for the strain used here. Although they had suffered both loss of material and structural distortions (see below) the isolated NPCs were pure enough to begin studies on their structure, composition, and physical properties.

The lack of any functional assay meant that this enrichment procedure was designed primarily to preserve only the detectable morphological features, and the dissociation of peripheral elements from the NPCs during their isolation would have been almost impossible to detect. The loss of at least one known NPC protein, NUP2, demonstrates that the isolated NPCs had in fact lost some components. However at least seven other known NPC proteins coenrich with the isolated NPCs, suggesting that they still retain a substantial proportion of the original NPC components.

The isolation procedures have allowed a preliminary investigation of yeast NPC ultrastructure. This has unequivocally confirmed that the yeast NPCs share the eightfold symmetry found in the NPCs of vertebrates. Complementary data gained from different fractions showed that the yeast NPC is also significantly smaller than vertebrate NPCs. This has been reported by others (Moor and Mühlethaler, 1963; Severs et al., 1976; Willison and Johnston, 1978). However the overall morphology and the diameters of the central pore and plug within appear to be conserved. The size conservation of the plug and central pore suggest that these features of the NPC are important for transport, as has been shown previously by thin section electron micrographs of both RNPs (Stevens and Swift, 1966; Mehlin et al., 1992) and nucleoplasmin-gold conjugates (Feldherr et al., 1984) in transit across the NPC. The NPCs in yeast may also have baskets and interbasket filaments comparable to those seen in Xenopus preparations. Much more detailed ultrastructural studies are in progress (with C. W. Akey).

The electron microscopical, biochemical, and immunological evidence indicates that the highly enriched NPC fraction is composed mainly of NPC proteins (Figs. 2, 3, and 4, Table I). That the NPC fraction is enriched enough to obtain sequences from a number of known NPC proteins implies that it is possible to obtain similar sequences from many more, as yet uncharacterized, NPC proteins. This is one of the main functions of this enrichment procedure, and indeed a number of these proteins are now being characterized. The clear presence of the plugs in the isolated NPCs also promises that much of the translocation machinery is still present. Experiments are in progress which will attempt to identify some of the components of this machinery. The eventual aim is to clone and sequence the genes for such NPC components, to allow their biochemical and genetic analysis.

The authors are greatly indebted to John Kilmartin, whose advice, support, and generosity were critical to this work, and who with Jan Fogg, provided most of the starting material used during the development of the enrichment procedure. Special thanks also go to: Chris Akey, who generously provided all the image analysis data and much helpful advice; Steve Burley, with whom many of the mass determination experiments were performed; Susan Wente, for numerous helpful suggestions and sharing of unpublished data; and Rick Wozniak, who provided HPLC and protein sequence data. Thanks also go to above people again and to John Aitchison, John Aris, Thelma Chen, Ann Ho, Mary Moore, Hiroshi Murakami, Chris Nichitta, Elena Sphicas, Caterina Strambio de Castillia, and Jun Sukegawa, for sharing much time, materials, data, and helpful advice.

M. P. Rout was supported by a fellowship from the Jane Coffin Childs Fund for Medical Research.

Received for publication 18 June 1993 and in revised form 17 August 1993.

References

Akey, C. W. 1989. Interactions and structure of the nuclear pore complex revealed by cryo-electron microscopy. *J. Cell Biol.* 109:955–970.

Akey, C. W. 1990. Visualization of transport-related configurations of the nuclear pore transporter. *Biophys. J.* 58:341–355.

Akey, C. W. 1992. The nuclear pore complex: a macromolecular transporter. *In* Nuclear Trafficking. C. Feldherr, editor. Academic Press, New York. 31–70.

Akey, C. W., and M. Radermacher. 1993. Architecture of the Xenopus nuclear pore complex revealed by three-dimensional cryo-electron microscopy. *J. Cell Biol.* 122:1–19.

Allen, J. L., and M. G. Douglas. 1989. Organization of the nuclear pore complex in Saccharomyces cerevisiae. *J. Ultrastruct. Mol. Struct. Res.* 102: 95–108.

Aris, J. P., and G. Blobel. 1988. Identification and characterization of a yeast nucleolar protein that is similar to a rat liver nucleolar protein. *J. Cell Biol.* 107:17–31.

Aris, J. P., and G. Blobel. 1989. Yeast nuclear envelope proteins cross react with an antibody against mammalian pore complex proteins. *J. Cell Biol.* 108:2059–2067.

Bornens, M., and J. C. Courvalin. 1978. Isolation of nuclear envelopes with polyanions. *J. Cell Biol.* 76:191–206.

Bradford, M. M. 1976. A rapid and sensitive method for the quantitation of microgram quantities of protein utilizing the principle of protein-dye binding. *Anal. Biochem.* 72:248–254.

Byers, B. 1981. Cytology of the yeast cell cycle. *In* Molecular Biology of the Yeast Saccharomyces: Life Cycle and Inheritance. J. N. Strathern, E. W. Jones, and J. R. Broach, editors. Cold Spring Harbor Laboratory, Cold Spring Harbor, New York. 59–96.

Cantor, C. R., and P. R. Schimmel. 1980. Biophysical Chemistry. Part II: Techniques for the study of biological structure and function. W. H. Freeman and Co., San Francisco, California.

Cardenas, M. E., T. Laroche, and S. M. Gasser. 1990. The composition and morphology of yeast nuclear scaffolds. *J. Cell Sci.* 96:439–450.

Carmo-Fonesca, M., H. Kern, and E. C. Hurt. 1991. Human nucleoporin p62 and the essential yeast nuclear pore protein NSP1 show sequence homology and a similar domain organization. *Eur. J. Cell Biol.* 55:17–30.

Chao, F.-C. 1957. Dissociation of macromolecular ribonucleoprotein of yeast. *Arch. Biochem. Biophys.* 70:426–431.

Chao, F.-C., and H. K. Schachman. 1956. The isolation and characterization of a macromolecular ribonucleoprotein from yeast. *Arch. Biochem. Biophys.* 61:220–230.

Cordes, V., I. Waizenegger, and G. Krohne. 1991. Nuclear pore complex glycoprotein p62 of Xenopus laevis and mouse: cDNA cloning and identification of its glycosylated region. *Eur. J. Cell Biol.* 55:31–47.

Dabauvalle, M. C., R. Benavente, and N. Chaly. 1988. Monoclonal antibodies to a Mr 68,000 pore complex glycoprotein interfere with nuclear protein uptake in Xenopus oocytes. *Chromosoma.* 97:193–197.

Davis, L. I., and G. Blobel. 1986. Identification and characterization of a nuclear pore complex protein. *Cell.* 45:699–709.

Davis, L. I., and G. Blobel. 1987. Nuclear pore complex contains a family of glycoproteins that includes p62: glycosylation through a previously unidentified cellular pathway. *Proc. Natl. Acad. Sci. USA.* 84:7552–7556.

Davis, L. I., and G. R. Fink. 1990. The NUP1 gene encodes an essential component of the yeast nuclear pore complex. *Cell.* 61:965–978.

Dwyer, N., and G. Blobel. 1976. A modified procedure for the isolation of a pore complex-lamina fraction from rat liver nuclei. *J. Cell Biol.* 70:581–591.

Eason, R. 1984. Analytical ultracentrifugation. *In* Centrifugation: a practical approach. D. Rickwood, editor. IRL Press Ltd., Oxford and Washington. 251–286.

Eddy, A. A., and D. H. Williamson. 1957. A method of isolating protoplasts from yeast. *Nature (Lond.).* 179:1252–1253.

Featherstone, C., M. K. Darby, and L. Gerace. 1988. A monoclonal antibody against the nuclear pore complex inhibits nucleocytoplasmic transport of protein and RNA in vivo. *J. Cell Biol.* 107:1289–1297.

Feldherr, C. M., E. Kallenbach, and N. Schultz. 1984. Movement of a karyophilic protein through the nuclear pores of oocytes. *J. Cell Biol.* 99:2216–2222.

Forbes, D. J. 1992. Structure and function of the nuclear pore complex. *Annu. Rev. Cell Biol.* 8:495–527.

Frank, J., B. Shimkin, and H. Dowse. 1981. SPIDER—a modular software system for electron image processing. *Ultramicroscopy.* 6:343–358.

Franke, W. W. 1974. Structure, biochemistry, and functions of the nuclear envelope. *Int. Rev. Cytol. Suppl.* 4:71–236.

Gerace, L., and B. Burke. 1988. Functional organization of the nuclear envelope. *Annu. Rev. Cell Biol.* 4:335–374.

Gerace, L., Y. Ottaviano, and C. Kondor-Koch. 1982. Identification of a major polypeptide of the nuclear pore complex. *J. Cell Biol.* 95:826–837.

Goldberg, M. W., and T. D. Allen. 1992. High resolution scanning electron microscopy of the nuclear envelope: demonstration of a new, regular, fibrous lattice attached to the baskets of the nucleoplasmic face of the nuclear pores. *J. Cell Biol.* 119:1429–1440.

Griffith, O. M. 1986. Techniques of preparative, zonal, and continuous flow ultracentrifugation. Beckman Handbook. Beckman Instruments, Inc., Palo Alto, CA. 1–50.

Harlow, E., and D. Lane. 1988. Antibodies: a laboratory manual. Cold Spring Harbor Laboratory, Cold Spring Harbor, New York. 1–726.

Hinshaw, J. E., B. O. Carragher, and R. A. Milligan. 1992. Architecture and design of the nuclear pore complex. *Cell.* 69:1133–1141.

Hurt, E. C., A. McDowall, and T. Schimmang. 1988. Nucleolar and nuclear envelope proteins of the yeast Saccharomyces cerevisiae. *Eur. J. Cell Biol.* 46:554–563.

Jarnik, M., and U. Aebi. 1991. Toward a more complete 3-D structure of the nuclear pore complex. *J. Struct. Biol.* 107:291–308.

Kilmartin, J. V., and J. Fogg. 1982. Partial purification of yeast spindle pole bodies. *In* Microtubules in Microorganisms. P. Cappuccinelli and N. R. Morris, editors. Marcel Dekker Inc., New York. 157–169.

Kilmartin, J. V., and A. E. Adams. 1984. Structural rearrangements of tubulin and actin during the cell cycle of the yeast Saccharomyces. *J. Cell Biol.* 98:922–933.

Laemmli, U. K. 1970. Cleavage of structural proteins during the assembly of the head of bacteriophage T4. *Nature (Lond.).* 227:680–685.

Loeb, J. D. J., L. I. Davis, and G. R. Fink. 1993. NUP2, a novel yeast nucleoporin, has functional overlap with other proteins of the nuclear pore complex. *Mol. Biol. Cell.* 4:209–222.

Maul, G. G. 1977. The nuclear and cytoplasmic pore complex: structure, dynamics, distribution, and evolution. *Int. Rev. Cytol. Suppl.* 5:75–186.

McEwen, C. R. 1967. Tables for estimating sedimentation through linear concentration gradients of sucrose solution. *Anal. Biochem.* 20:114–149.

Mehlin, H., B. Daneholt, and U. Skoglund. 1992. Translocation of a specific premessenger ribonucleoprotein particle through the nuclear pore studied with electron microscope tomography. *Cell.* 69:605–613.

Miller, M., M. K. Park, and J. A. Hanover. 1991. Nuclear pore complex: structure, function, and regulation. *Physiol. Rev.* 71:909–949.

Moor, H., and K. Mühlethaler. 1963. Fine structure in frozen-etched yeast cells. *J. Cell Biol.* 17:609–627.

Mortimer, R. K., and J. R. Johnston. 1986. Genealogy of principal strains of the yeast genetic stock center. *Genetics.* 113:35–43.

Nehrbass, U., and E. C. Hurt. 1992. Nuclear transport and nuclear pores in yeast. *Antonie Van Leeuwenhoek.* 62:3–14.

Nehrbass, U., H. Kern, A. Mutvei, H. Horstmann, B. Marshallsay, and E. C. Hurt. 1990. NSP1: a yeast nuclear envelope protein localized at the nuclear pores exerts its essential function by its carboxy-terminal domain. *Cell.* 61:979–989.

Nelson, D. A., W. R. Beltz, and R. L. Rill. 1977. Chromatin subunits from baker's yeast: isolation and partial characterization. *Proc. Natl. Acad. Sci. USA.* 74:1343–1347.

Pain, D., H. Murakami, and G. Blobel. 1990. Identification of a receptor for protein import into mitochondria. *Nature (Lond.).* 347:444–449.

Park, M. K., M. D'Onofrio, M. C. Willingham, and J. A. Hanover. 1987. A monoclonal antibody against a family of nuclear pore proteins (nucleoporins): O-linked N-acetylglucosamine is part of the immunodeterminant. *Proc. Natl. Acad. Sci. USA.* 84:6462–6466.

Radu, A., G. Blobel, and R. W. Wozniak. 1993. Nup155 is a novel nuclear pore complex protein that contains neither repetitive sequence motifs nor reacts with WGA. *J. Cell Biol.* 121:1–10.

Reichelt, R., A. Holzenburg, E. L. J. Buhle, M. Jarnik, A. Engel, and U. Aebi. 1990. Correlation between structure and mass distribution of the nuclear pore complex and of distinct pore complex components. *J. Cell Biol.* 110:883–894.

Richardson, W. D., A. D. Mills, S. M. Dilworth, R. A. Laskey, and C. Dingwall. 1988. Nuclear protein migration involves two steps: rapid binding at the nuclear envelope followed by slower translocation through nuclear pores. *Cell.* 52:655–664.

Rickwood, D. 1984. The theory and practice of centrifugation. *In* Centrifugation: A Practical Approach. D. Rickwood, editor. IRL Press Inc., Oxford and Washington. 1–43.

Ris, H. 1990. Application of low voltage, high resolution SEM in the study of complex intracellular structures. *Proceedings of the XIIth International Congress for Electron Microscopy.* 18–19.

Ris, H. 1991. The three dimensional structure of the nuclear pore complex as seen by high voltage electron microscopy and high resolution low voltage scanning electron microscopy. *EMSA Bulletin.* 21:54–56.

Rout, M. P., and J. V. Kilmartin. 1990. Components of the yeast spindle and spindle pole body. *J. Cell Biol.* 111:1913–1927.

Rout, M. P., and J. V. Kilmartin. 1993. Preparation of yeast spindle pole bodies. *In* Cell Biology: A Biology Handbook. J. E. Celis, editor. Academic Press, New York. In press.

Rozijn, T. H., and G. J. M. Tonino. 1964. Studies on the yeast nucleus. I. The isolation of nuclei. *Biochim. Biophys. Acta.* 91:105–112.

Scheer, U. 1972. Ultrastructure of the nuclear envelope of amphibian oocytes. IV. Chemical nature of the nuclear pore complex material. *Z. Zellforsch Mikrosk. Anat.* 127:127–148.

Severs, N. J., E. G. Jordan, and D. H. Williamson. 1976. Nuclear pore absence from areas of close association between nucleus and vacuole in synchronous yeast cultures. *J. Ultrastruct. Res.* 54:374–387.

Snow, C. M., A. Senior, and L. Gerace. 1987. Monoclonal antibodies identify a group of nuclear pore complex glycoproteins. *J. Cell Biol.* 104:1143–1156.

Starr, C. M., M. D'Onofrio, M. K. Park, and J. A. Hanover. 1990. Primary sequence and heterologous expression of nuclear pore glycoprotein p62. *J. Cell Biol.* 110:1861–1871.

Stevens, B. J., and H. Swift. 1966. RNA transport from nucleus to cytoplasm in Chironomus salivary glands. *J. Cell Biol.* 31:55–77.

Sukegawa, J., and G. Blobel. 1993. A nuclear pore complex protein that contains zinc finger motifs, binds DNA, and faces the nucleoplasm. *Cell.* 72:29–38.

te Heesen, S., R. Rauhut, R. Aebersold, J. Abelson, M. Aebi, and M. W. Clark. 1991. An essential 45 kDa yeast transmembrane protein reacts with anti-nuclear pore antibodies: purification of the protein, immunolocalization and cloning of the gene. *Eur. J. Cell Biol.* 56:8–18.

Thomas, J. O., and V. Furber. 1976. Yeast chromatin structure. *FEBS (Fed. Eur. Biochem. Soc.) Letts.* 66:274–280.

Towbin, H., T. Staehlin, and J. Gordon. 1979. Electrophoretic transfer of proteins from polyacrylamide gels to nitrocellulose sheets: procedure and some applications. *Proc. Natl. Acad. Sci. USA.* 76:4350–4354.

Unwin, P. N., and R. A. Milligan. 1982. A large particle associated with the perimeter of the nuclear pore complex. *J. Cell Biol.* 93:63–75.

Wente, S. R., M. P. Rout, and G. Blobel. 1992. A new family of yeast nuclear pore complex proteins. *J. Cell Biol.* 119:705–723.

Willison, J. H., and G. C. Johnston. 1978. Altered nuclear pore diameters in G1-arrested cells of the yeast Saccharomyces cerevisiae. *J. Bacteriol.* 136:318–323.

Wimmer, C., V. Doye, P. Grandi, U. Nehrbass, and E. C. Hurt. 1992. A new subclass of nucleoporins that functionally interact with the nuclear pore protein NSP1. *EMBO (Eur. Mol. Biol. Org.) J.* 11:5051–5061.

Wozniak, R. W., E. Bartnik, and G. Blobel. 1989. Primary structure analysis of an integral membrane glycoprotein of the nuclear pore. *J. Cell Biol.* 108:2083–2092.